Hindawi
Cellular Microbiology
Volume 2022, Article ID 8612113, 18 pages
https://doi.org/10.1155/2022/8612113

Research Article

Guanylate-Binding Protein 1 Regulates Infection-Induced Autophagy through TBK1 Phosphorylation

Miyako Hikichi, Hirotaka Toh, Atsuko Minowa-Nozawa, Takashi Nozawa, and Ichiro Nakagawa

Department of Microbiology, Graduate School of Medicine, Kyoto University, Yoshida-Konoe-cho, Sakyo-ku, Kyoto 606-8501, Japan

Correspondence should be addressed to Takashi Nozawa; nozawa.takashi.4r@kyoto-u.ac.jp
and Ichiro Nakagawa; nakagawa.ichiro.7w@kyoto-u.ac.jp

Received 26 February 2022; Revised 16 March 2022; Accepted 22 March 2022; Published 29 May 2022

Academic Editor: Jayaprakash Kolla

Invading bacteria can be degraded by selective autophagy, known as xenophagy. Recent studies have shown that the recruitment of autophagy adaptor proteins such as p62 to bacteria and its regulation by activated TANK-binding kinase 1 (TBK1) are required to overcome bacterial infection. However, the detailed molecular mechanisms behind this are not yet fully understood. Here, we show that the human guanylate-binding protein (GBP) family, especially GBP1, directs xenophagy against invading Group A *Streptococcus* (GAS) by promoting TBK1 phosphorylation. GBP1 exhibits a GAS-surrounding localization response to bacterially caused membrane damage mediated by the membrane damage sensor galectin-3. We found that GBP1 knockout attenuated TBK1 activation, followed by reduced p62 recruitment and lower bactericidal activity by xenophagy. Furthermore, GBP1-TBK1 interaction was detected by immunoprecipitation. Our findings collectively indicate that GBP1 contributes to GAS-targeted autophagy initiated by membrane damage detection by galectin-3 via TBK1 phosphorylation.

1. Introduction

During bacterial infection, interferons (IFNs) activate the expression of a series of "interferon-stimulated genes" to trigger the immune response pathway [1, 2]. These genes include members of the guanylate-binding protein (GBP) family, which has 11 homologs in mice and 7 in humans and has been reported to exert antipathogenic effects in both species [3, 4]. For instance, mouse GBP7 interacts with NADPH oxidase components, promoting *Listeria monocytogenes* or *Mycobacterium bovis* BCG degradation [5]. In contrast, it has been reported that human GBP1 targets lipopolysaccharide (LPS), a component of the cell wall of Gram-negative bacteria. Polymerized human GBP1 binds to LPS to promote bacterial outer membrane degradation and support caspase-4 activation required for inflammasome formation [3, 6–8]. Additionally, human GBP1 regulates GBP2, GBP3, and GBP4 recruitment to *Shigella flexneri* and inhibits the motility of this bacterium when it attempts to degrade GBPs via the ubiquitin-proteasome system [9–11]. Thus, the GBP family is involved in the immune response of host cells to bacteria in multiple ways.

Another immune response during bacterial infection is autophagy. Autophagy is a widely conserved intracellular degradation mechanism. As its name suggests, selective autophagy mediates the degradation of specific components and contributes to the maintenance of intracellular homeostasis by degrading depolarized mitochondria, damaged lysosomes, and aggregated proteins [12, 13]. Autophagy has also been reported to function as an immune response by degrading invading bacteria in a process known as "xenophagy." It is triggered by the detection of invading bacteria by the host. First, the host labels the pathogen via E3 ligase-mediated ubiquitination, the mechanisms of which have recently been a focus of study [14–16]. The next step is for the host to crosslink the ubiquitinated bacteria to the autophagosome precursor, the isolation membrane. The adaptor proteins NDP52, p62, NBR1, TAX1BP1, and OPTN

are responsible for this process by entrapping the bacteria via the crosslinking of ubiquitin and ATG8 (LC3/GABARAP) anchored to the isolation membrane [17]. TANK-binding kinase 1 (TBK1) phosphorylates the adaptor proteins NDP52, p62, and OPTN to promote their binding to ubiquitin after its activation through bacterial infection. TBK1 activation evoked by bacterial remnants such as DNA and LPS has been reported [18]. We also recently reported that intracellular signaling with Ca2+ induced by bacterial toxin facilitates TBK1 activation during bacterial infection [19]. However, how host sensors recognize bacterial infection and induce TBK1's activation remains unclear.

Both the GBP family and xenophagy are involved in immune responses, and their interaction is also gradually being reported. For example, in the human monocytic cell THP1, human GBP1 or GBP2 knockdown increases monomeric ATG5 and ATG12, whose complex is essential for autophagy induction and associated with the degradation of *Chlamydia* [20]. Furthermore, mouse GBP1 was reported to contribute to the degradation of *Listeria* and *BCG* by binding to p62 [5]. However, the functions of the GBP family differ among cell types and pathogens [5, 6, 21], so this family remains incompletely understood.

In this study, we examine the functions of the GBP family in xenophagy induced by Group A *Streptococcus* (GAS), a typical human pathogen that causes various severe infectious diseases [22]. We show that the recruitment of GBP1 to bacteria mediated by the recognition of membrane damage by the host is critical for xenophagy. Furthermore, we identify GBP1 as a regulator of TBK1 phosphorylation and clarify the GBP1-TBK1 axis.

1.1. GBP1 Is Localized at the Autophagosome around GAS in a GTPase Activity- and Lipidation-Dependent Manner. To investigate whether GBP family members are involved in GAS-induced autophagy, we observed their localization during GAS infection. HeLa cells overexpressing mCherry-LC3 as an autophagosomal marker [23] and GFP-fused members of the GBP family were infected with the GAS strain JRS4 for 4 h, followed by observation using confocal microscopy. We first checked the localization of the GBPs. Of the seven human GBPs, GBP1, GBP2, and GBP4 were colocalized with LC3 around the GAS, reflecting an autophagosome containing GAS [23] (Figure 1(a)). GBP1 had the most pronounced localization among these GBPs, which reached almost 40% of total autophagosomes surrounding GAS, which was twice that of GBP2, the second most common GBP (Figure 1(b)). It has been reported that GBP1 interferes with the expansion of infection by inhibiting bacterial cell-to-cell spread in epithelial cells. Additionally, other reports have demonstrated that human GBP1 has high homology with mouse GBP2, contributing to bacterial degradation [24, 25]. For these reasons, we decided to focus on the dynamics of GBP1 in GAS infection.

To identify the functional regions of GBP1 required for the localization to GAS, we constructed mutants with impairments in GTPase and GDPase activity, membrane binding ability, and an altered ubiquitination site. For both R48A (GTPase-deficient) and D184N (GTPase-constitutively active) [26, 27], the localization of GBP1 to GAS was completely abolished, whereas for G68A (GDPase-deficient) [28], it was drastically but not completely reduced (Figures 1(c) and 1(d)). These results suggest that nucleotide recycling, especially that of GTP and GDP, is critical for the recruitment. Moreover, C589S and ΔCTIS, prenylation-deficient mutants [29, 30], did not exhibit recruitment to the bacteria (Figures 1(c) and 1(d)), implying that GBP1 is localized on the host membrane because prenylation is critical for membrane binding. In contrast, for the K382R mutant with mutation of a ubiquitination site [31], there was only a slight decrease in its localization at the bacteria (Figures 1(c) and 1(d)). These results indicate that GBP1 is recruited in a manner dependent on its nucleotide hydrolysis activity and lipidation.

1.2. GBP1 Localization Does Not Depend on the Canonical Autophagy Pathway. A previous report demonstrated that ATG5-knockout mouse embryonic fibroblasts (MEFs), which are unable to undergo autophagy, showed a drastic reduction of mouse GBP2 localization around *Toxoplasma* and *Chlamydia* [32]. Therefore, we wanted to clarify whether human GBP1 localization to GAS is under the control of ATG5, the canonical autophagy regulator. Among infected cells, the rate of cells containing GBP1-positive bacteria was slightly increased in ATG5-knockout HeLa cells, but this did not reach significance (Figure 1(e)). Therefore, we concluded that GBP1 localization to GAS is independent of canonical autophagy.

1.3. Recognition of Membrane Rupture by Galectin-3 Is Required for GBP1 Localization to GAS. We next investigated how GBP1 is recruited to GAS. During infection, GAS invades epithelial cells via endocytosis and then escapes into the cytosol by secreting the pore-forming toxin streptolysin O (SLO) [23]. Cells detect the pore via galectin-3, and their autophagy is induced [33]. A previous study reported that, under *Legionella pneumophila* or *Yersinia pseudotuberculosis* infection, mouse GBP2 is recruited to the bacteria in a pore-forming protein-dependent manner [25]. To examine whether membrane damage caused by GAS infection triggers GBP1 recruitment, we infected SLO-deficient GAS and observed GBP1 localization. We found that infection by SLO-deficient GAS resulted in the complete abolition of GBP1 recruitment (Figure 2(a)). As for pore detection by galectin-3, GBP1 was found to colocalize with galectin-3 around GAS (Figure 2(b)). Furthermore, GBP1 recruitment was reduced in galectin-3-knockout cells (Figures 2(c) and 2(d)), while this reduction was recovered by galectin-3 overexpression (Figure 2(e)). In contrast to GBP1, there were no changes in the localization of GBP2 and GBP4 in galectin-3-knockout cells (Supplementary Figure 1A). These findings suggest that GBP1 recruitment to GAS is dependent on pore formation by SLO and the detection of membrane damage by galectin-3. Mouse GBP2 has been reported to interact with galectin-3 in a manner dependent on membrane damage [25], so we next examined whether human GBP1 and galectin-3 interact. Immunoprecipitation revealed that GBP1 interacted with galectin-3, which was

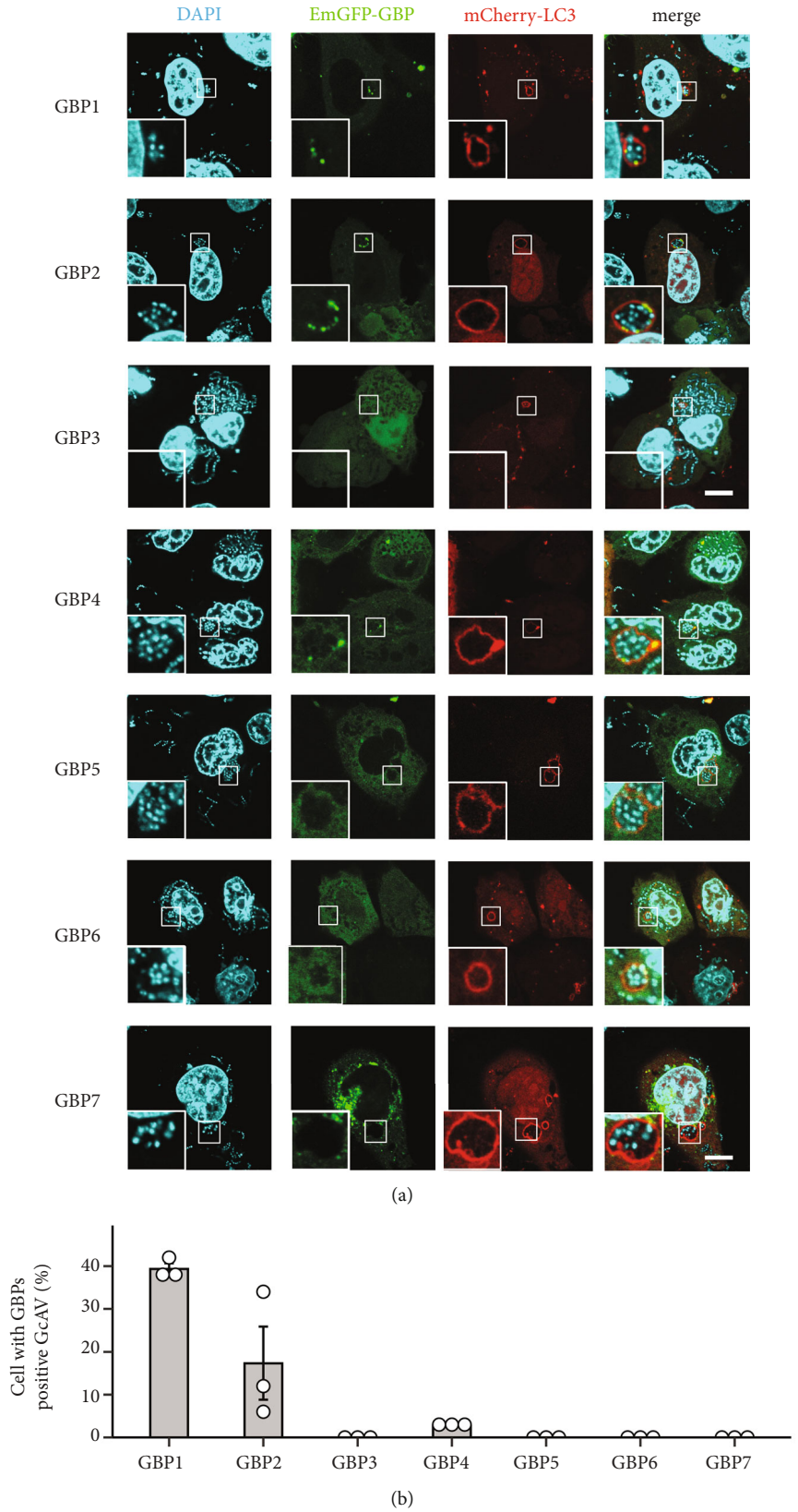

Figure 1: Continued.

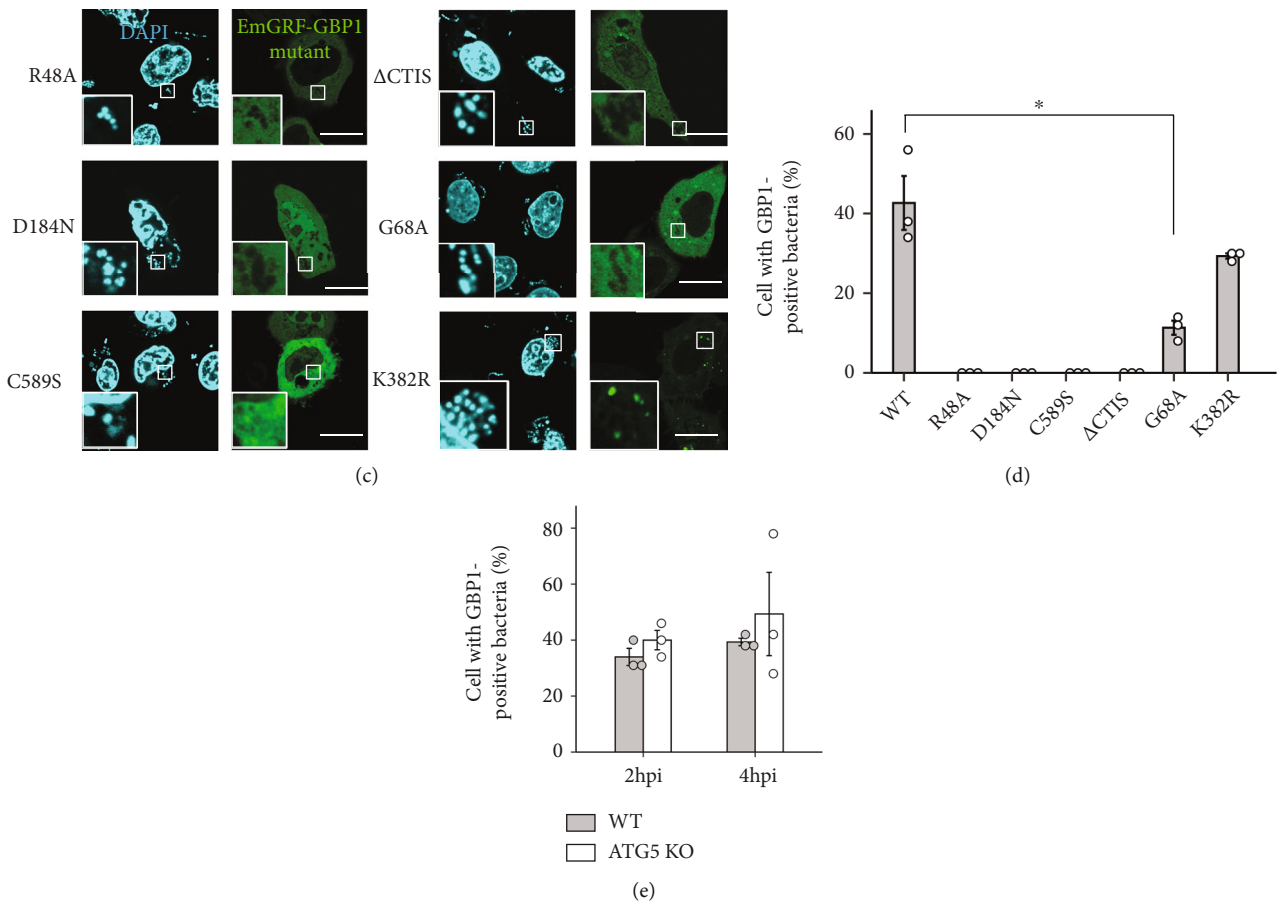

Figure 1: GBP1 localization around the autophagosome depending on guanine nucleotide recycling and lipidation. (a) Confocal micrographs of the GBP family around an autophagosome in GAS-infected cells. HeLa cells expressing the indicated EmGFP-GBPs (green) and mCherry-LC3 (red) were infected with GAS for 4 h. Cellular and bacterial DNA was stained with DAPI (cyan). All images are representative of three independent experiments. Insets: enlargements of the indicated areas. Scale bar: 10 μm. (b) Quantification of cells containing the GBP-positive autophagosome among GAS-infected cells; cells were manually counted by observing immunofluorescence using confocal microscopy. Data are presented as the mean ± SD from three independent experiments (100 infected cells were examined in each experiment). Of the seven GBP homologs, only data of autophagosome-localized GBPs are shown. (c) Confocal micrograph of GBP1 mutants and the autophagosome in GAS-infected cells. HeLa cells cotransfected with EmGFP-GBP1 mutants and mCherry-LC3 were infected with GAS for 4 h. Cellular and bacterial DNA was stained with DAPI. All images are representative of three independent experiments. Insets: enlargements of indicated areas. Scale bar: 10 μm. (d) Quantification of cells containing the GBP1 mutant-positive autophagosome in GAS-infected cells. Cells were manually counted by observing immunofluorescence using confocal microscopy. Data are presented as the mean ± SD from three independent experiments (50 infected cells were examined in each experiment). Asterisks indicate statistically significant differences ($^*p < 0.05$) as determined by two-tailed Student's t-test. (e) Quantification of cells containing GBP1-positive GAS in HeLa WT and ATG5-knockout cells [57]. Cells were manually counted by observing immunofluorescence using confocal microscopy. Data are presented as the mean ± SD from three independent experiments (50 infected cells were examined in each experiment).

enhanced by GAS infection (Supplementary Figure 2A, 4th and 5th lanes from the left). Interestingly, other galectins that have been reported to be involved in autophagy induced by GAS infection also showed interaction with GBP1 to a lesser extent than galectin-3 (Supplementary Figure 2A). These results suggest that GBP1-galectin-3 interaction is especially potentiated by GAS infection, which leads to the recruitment of GBP1 to GAS.

1.4. GBP1 Is Recruited to Not Only Bacteria But Also Damaged Lysosome. We additionally evaluated whether other types of membrane damage can alter the localization of GBP1. $_L$-Leucyl-$_L$-leucine methyl ester (LLOMe) induces damage to lysosomal membranes, which is recognized by galectin-3, leading to lysosomal degradation called lysophagy [34]. It has been reported that LLOMe treatment in human embryonic kidney (HEK) 293T cells induced GBP1 recruitment close to galectin-3 [25], but this was not confirmed in HeLa cells. We also found that GBP1 colocalized with galectin-3-positive puncta upon treatment with LLOMe, reflecting recruitment to the ruptured lysosomes (Figure 2(f)). As in bacterial infection, this indicates that

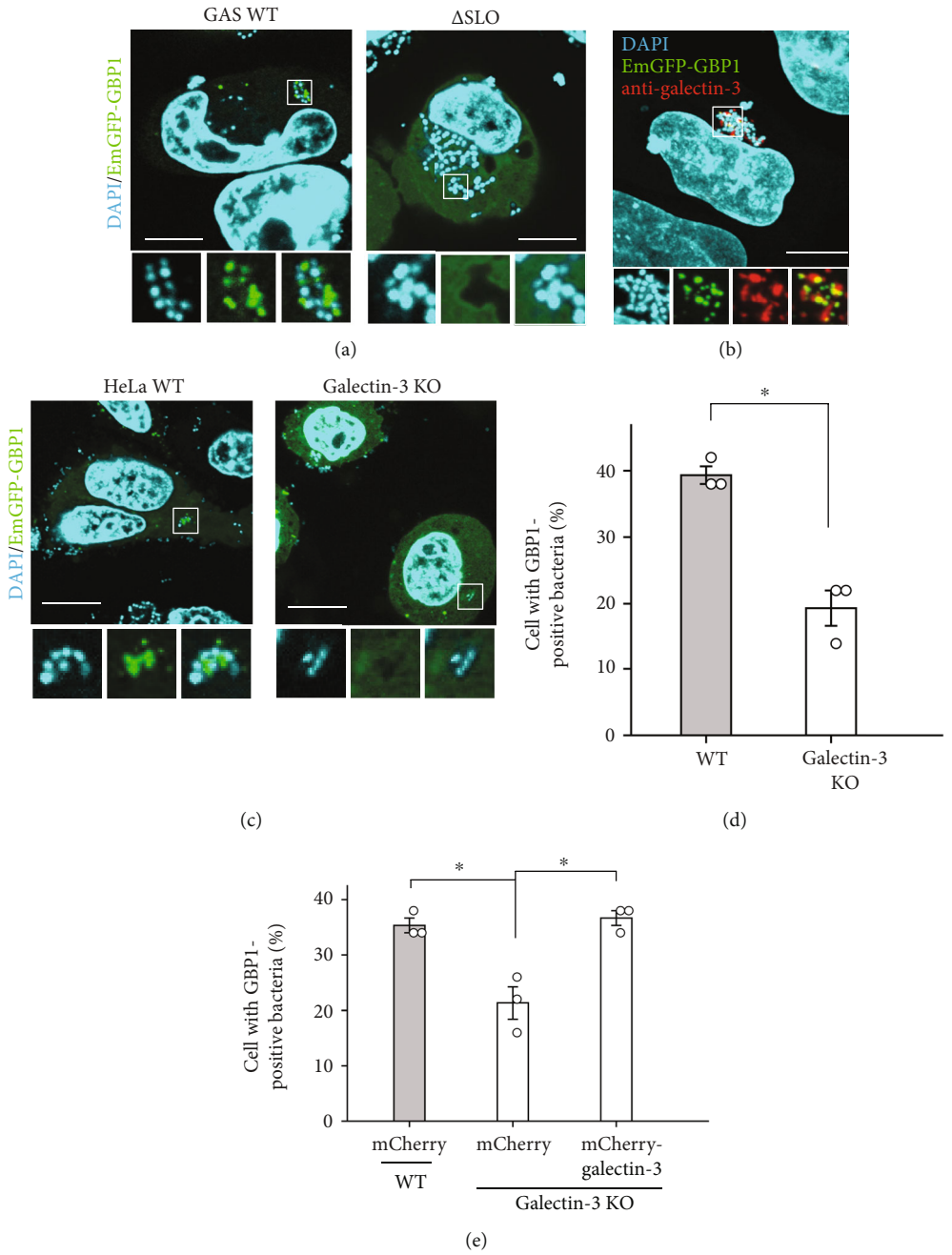

Figure 2: Continued.

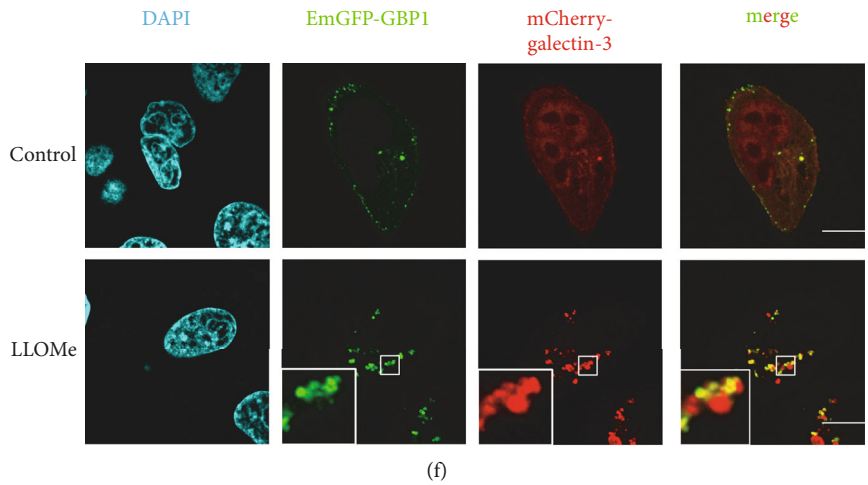

Figure 2: GBP1 localization is dependent on membrane damage and its recognition by galectin-3. (a) Confocal micrographs of GBP1 localization with infection of GAS wild type (WT) or *slo* deletion mutant. HeLa cells overexpressing EmGFP-GBP1 were infected with the indicated bacteria for 4 h. Cellular and bacterial DNA was stained with DAPI. An overview of the merging of all channels (top) and a magnified view of each channel and that of the merging of all channels (bottom) are shown. Scale bar: 10 μm. (b) GBP1 and galectin-3 localization in GAS-infected cells. HeLa cells were transfected with EmGFP-GBP1. After GAS infection for 4 h, cells were stained with anti-galectin-3 and DAPI. An overview of the merging of all channels (top) and a magnified view of each channel and that of the merging of EmGFP-GBP1 and galectin-3 (bottom) are shown. Scale bar: 10 μm. (c) GBP1 recruitment in galectin-3-knockout cells [50]. WT and galectin-3-knockout (KO) HeLa cells were transfected with EmGFP-GBP1, followed by GAS infection for 4 h. Cellular and bacterial DNA was stained with DAPI. An overview of the merging of all channels (top) and a magnified view of each channel and that of the merging of DAPI and EmGFP-GBP1 (bottom) are shown. Scale bar: 10 μm. (d) Quantification of GBP1 recruitment in (c). Cells were manually counted by observing immunofluorescence using confocal microscopy. Data are presented as the mean ± SD from three independent experiments (100 infected cells were examined in each experiment). Asterisks indicate statistically significant differences ($^*p < 0.05$) as determined by two-tailed Student's *t*-test. (e) Quantification of GBP1 recruitment in galectin-3 complementation. Cells were transfected with the indicated plasmid, infected with GAS for 4 h, and stained with DAPI. Cells were manually counted by observing immunofluorescence using confocal microscopy. Data are presented as the mean ± SD from three independent experiments (50 infected cells were examined in each experiment). Asterisks indicate statistically significant differences ($^*p < 0.05$) as determined by two-tailed Student's *t*-test. (f) GBP1 recruitment to the damaged lysosome after $_L$-leucyl-$_L$-leucine methyl ester (LLOMe) treatment. HeLa cells transfected with the indicated plasmids were treated with 0.5 mM LLOMe for 2 h. Cellular and bacterial DNA was stained with DAPI. Scale bar: 10 μm.

GBP1 is recruited to the damaged membrane. These findings together suggest that membrane damage by SLO and its recognition by galectin-3 are critical for the localization of GBP1 to GAS.

1.5. GBP1 Is Required for Autophagosome Formation Dependent on Its Localization to Bacteria. To date, we have focused on GBP1 dynamics during GAS infection. Now, we move on to investigating whether GBP1 is involved in autophagosome formation. We generated GBP1-knockout HeLa cells using CRISPR/Cas9 genome editing (Figure 3(a)). The autophagosome formation response to GAS infection was partially but significantly decreased in these knockout cells (Figures 3(b) and 3(c)). To confirm the involvement of GBP1 in autophagosome formation, we rescued GBP1 expression in GBP1-knockout cells. As expected, autophagosome formation was recovered by GBP1 expression (Figure 3(d)). We also evaluated autophagosome maturation using LAMP1, a lysosome marker, because autophagosomes fuse with lysosomes to degrade their components. As with autophagosome formation, GBP1 knockout reduced LAMP1 localization around GAS, while this recruitment was recovered by GBP1 complementation (Supplementary Figures 3A and 3B). These findings indicate that GBP1 is involved in autophagosome formation and thereby affects subsequent autophagosome maturation.

Figure 1 clarifies that GBP1 localizes to GAS in a manner dependent on its nucleotide-binding cycling and prenylation at the C-terminus, so we hypothesized that GBP1 regulates the autophagosome formation against invading GAS by being recruited close to bacteria. To examine this, we used GBP1 mutants lacking the ability to be recruited to GAS. The reduction of GAS-surrounding autophagosomes in GBP1-knockout cells was recovered by the artificial overexpression of GBP1 (Figure 3(d)). However, none of the GBP1 mutants tested in this experiment recovered autophagosome formation with such overexpression (Figure 3(d)), suggesting that GBP1 regulates autophagosome formation upon GAS infection by recruitment to the bacteria.

We also examined the effects of GBP1 knockout on bacterial killing activity by xenophagy. Because human epithelial lung carcinoma A549 cells efficiently eliminate intracellular GAS through xenophagy, we used A549 cells to investigate the bactericidal activity by examining intracellular viable

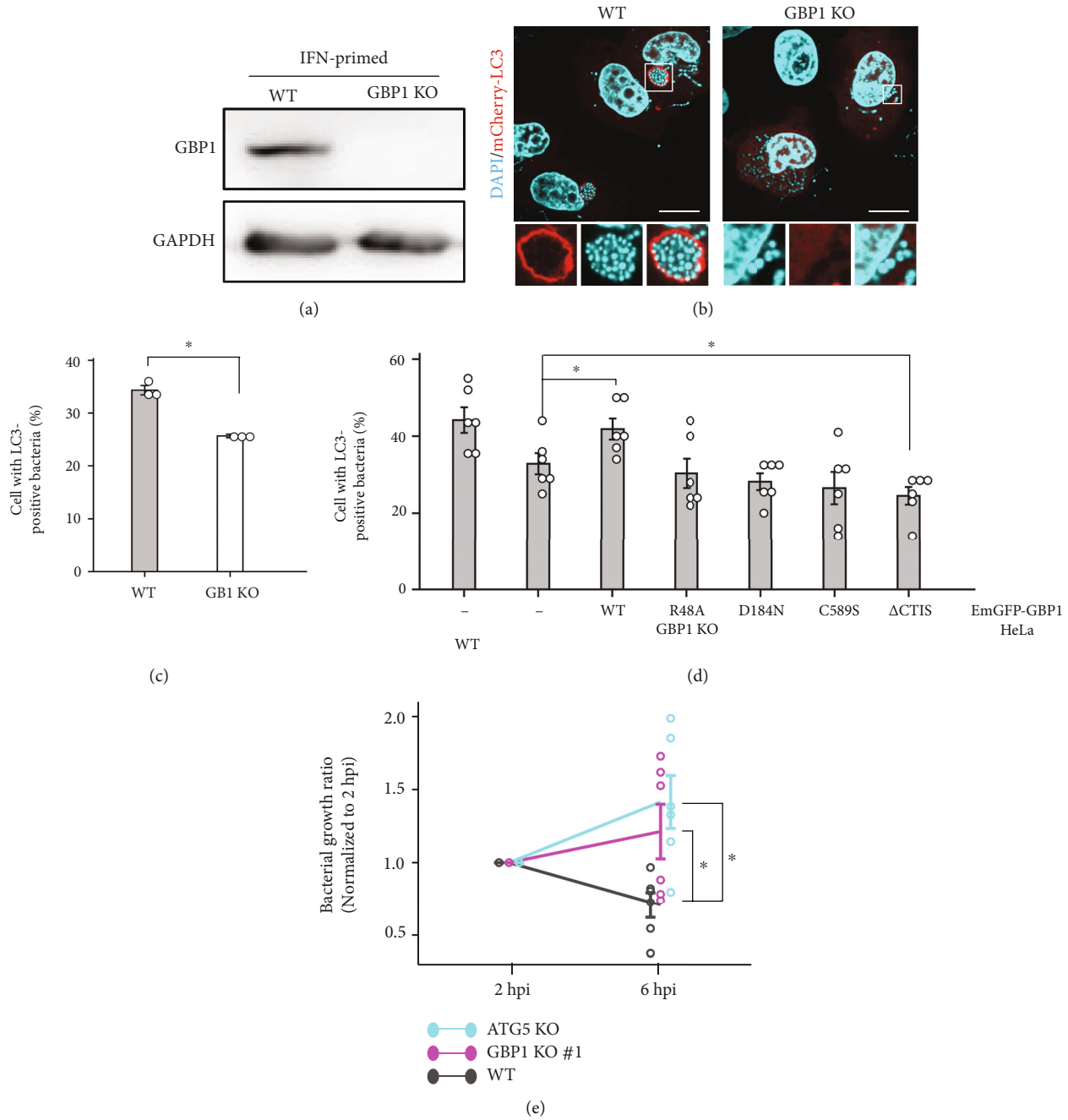

Figure 3: GBP1 is required for autophagosome formation in a localization-dependent manner. (a) GBP1-KO cells were generated using the CRISPR/Cas9 gene editing system. HeLa WT and GBP1-KO cells were treated with 20 ng/mL IFN-γ for 24 h and then collected to confirm GBP1 expression by immunoblotting. (b) Autophagosome formation in HeLa WT and GBP1 KO cells. Cells were transfected with mCherry-LC3 as an autophagosome marker and then infected with GAS for 4 h. An overview of the merging of all channels (top) and a magnified view of each channel and that of the merging of all channels (bottom) are shown. All images are representative of three independent experiments. Scale bar: 10 μm. (c) Autophagosome formation rate in GAS-infected cells. Data are presented as the mean ± SD from three independent experiments (100 infected cells were manually counted in each experiment). Asterisks indicate statistically significant differences ($^*p < 0.05$) as determined by two-tailed Student's t-test. (d) Percentage of autophagosome formation in GBP1-KO HeLa cells under conditions of GBP1 mutant overexpression. HeLa WT and GBP1-KO cells were transfected with EmGFP, EmGFP-GBP1 intact, or mutants. Data are presented as mean ± SD from three independent experiments (100 infected cells were manually counted in each experiment). Asterisks indicate statistically significant differences ($^*p < 0.05$) as determined by two-tailed Student's t -test. (e) Viability of GAS in A549 WT, GBP1-KO #1, and ATG5-KO cells. In each experiment, triplicate samples were used and colonies were counted manually. Data are presented as the mean ± SD from four independent experiments. Asterisks indicate statistically significant differences ($^*p < 0.05$) as determined by two-tailed Student's t-test. The same data of GBP1 KO #2 are shown in Supplementary Figure 2D.

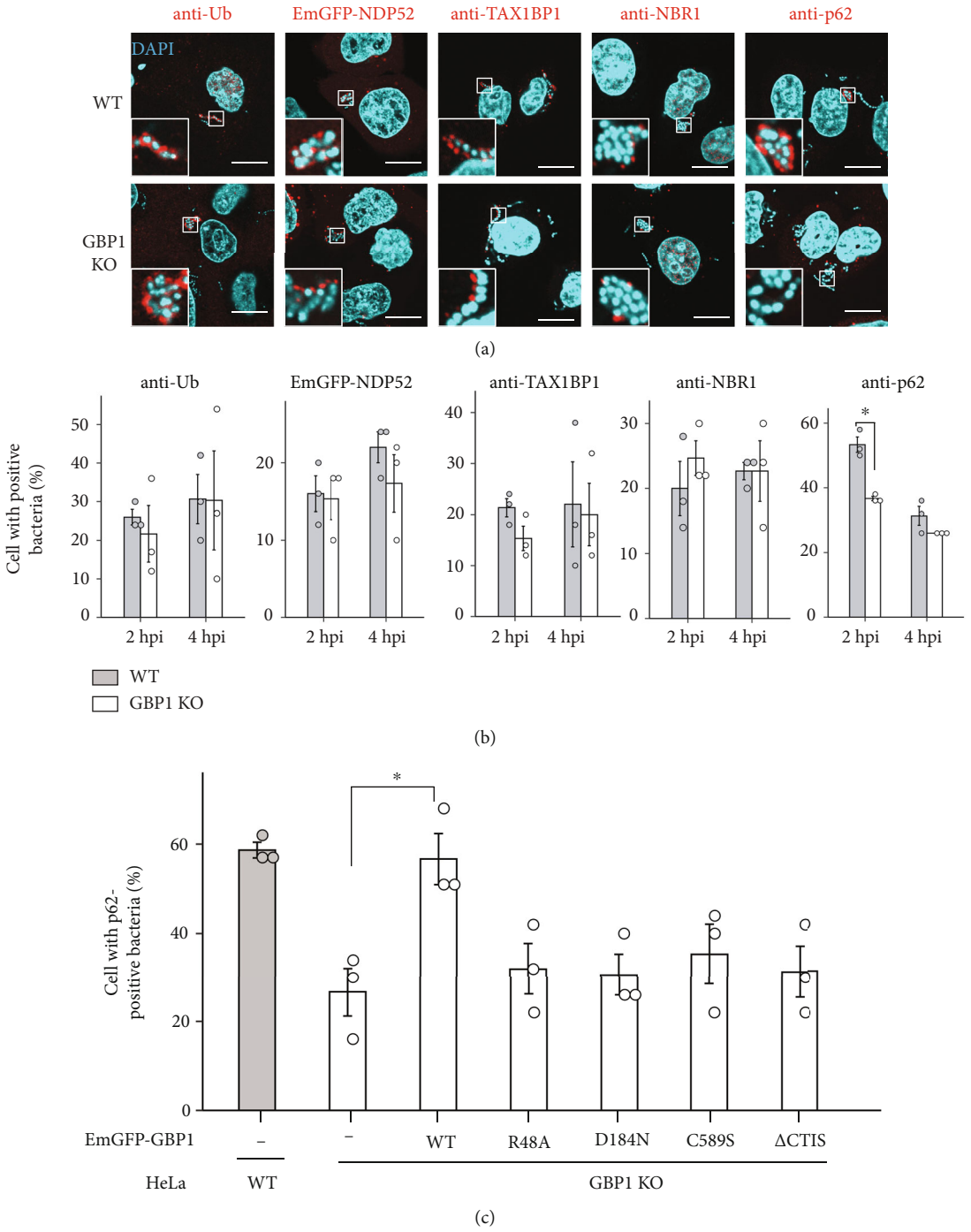

Figure 4: Continued.

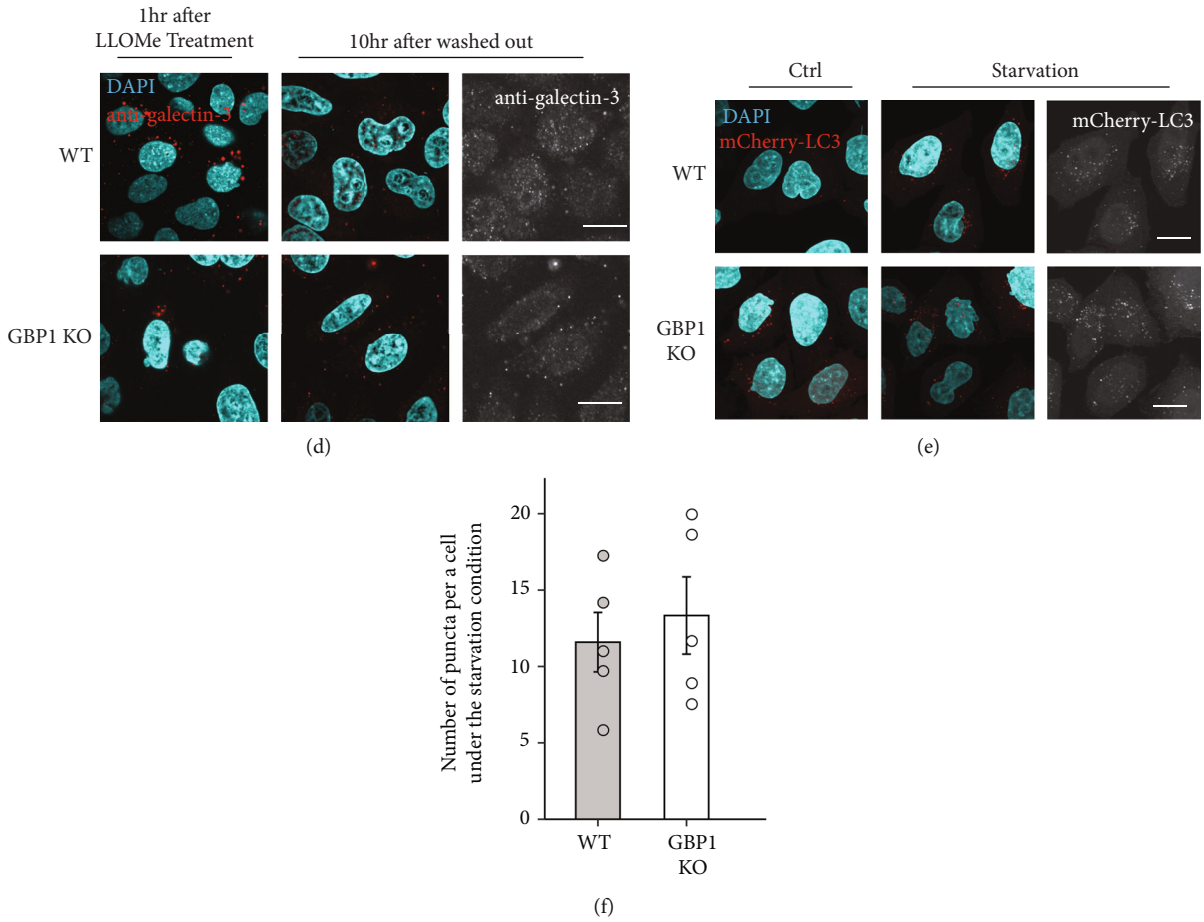

Figure 4: GBP1 is involved in p62 recruitment to GAS. (a) Recruitment of autophagy-related proteins to invading GAS. Cells were transfected with the indicated plasmid prior to infection or labeled with antibodies for the indicated protein after infection. Cellular and bacterial DNA was stained with DAPI. All images are representative of three independent experiments for 2 h of infection. Insets: enlargements of indicated areas. Scale bar: 10 μm. (b) Percentage of indicated protein recruitment to GAS in (a). Cells were infected with GAS for 2 or 4 h. Data are presented as the mean ± SD from three independent experiments (100 infected cells were manually counted in each experiment). Asterisks indicate statistically significant differences ($^*p < 0.05$) as determined by two-tailed Student's t-test. (c) Percentage of p62 recruitment to GAS under conditions of GBP1 mutant overexpression. HeLa WT and GBP1-KO cells were transfected with EmGFP, EmGFP- GBP1 intact, or mutants. Data are presented as mean mean ± SD from three independent experiments (100 infected cells were manually counted in each experiment). Asterisks indicate statistically significant differences ($^*p < 0.05$) as determined by two-tailed Student's t-test. (d) Degradation of the lysosome damaged by LLOMe treatment. HeLa cells were treated with 0.5 mM LLOMe for 2 h. Damaged lysosomes were labeled with an anti-galectin-3 antibody. Scale bar: 10 μm. (e) Starvation-induced autophagosome formation in HeLa WT and GBP1-KO cells. Indicated cells stably expressing mCherry-LC3 as an autophagosome marker were incubated in the medium without serum for 2 h. All images are representative of three independent experiments. Scale bar: 10 μm. (f) Quantification of mCherry-LC3 puncta in (e). At least 30 cells were obtained from five randomly selected fields in each condition (repeated three times). Puncta were counted automatically using the Analyze Particle plugin in Fiji software (ImageJ; National Institutes of Health).

bacteria after infection. First, we checked GBP family localization in A549 during GAS infection. As in HeLa cells, GBP1, GBP2, and GBP4 were localized at autophagosomes surrounding GAS (Supplementary Figure 4A). Therefore, we moved to generate GBP1-knockout cells using A549. Two different deletion strains were established for eliminating clonal effect from the assay (Supplementary Figures 4B and 4C). We infected these cells with GAS and determined the bacterial survival at 6 h postinfection. As shown in Figure 3(e), in wild-type A549 cells, the intracellular survival of GAS was reduced by about half from 2 to 6 h, while this did not occur in ATG5-knockout cells, a mutant with severe deficiency in autophagy [35] (Supplementary Figure 4D). In GBP1-knockout cells, the number of surviving bacteria at 6 h after infection was significantly higher than that in WT cells (Figure 3(e), Supplementary Figure 4E), supporting the assertion that GBP1 contributes to the bacterial killing through the autophagy pathway.

To confirm definitively that GBP1 is involved in autophagosome formation in A549 cells as well as HeLa cells, we also observed autophagosomes surrounding GAS in A549 cells. GBP1 deletion decreased the rate of autophagosome formation, which was recovered by GBP1 complementation, the same as in HeLa cells (Supplementary Figure 4F), supporting our

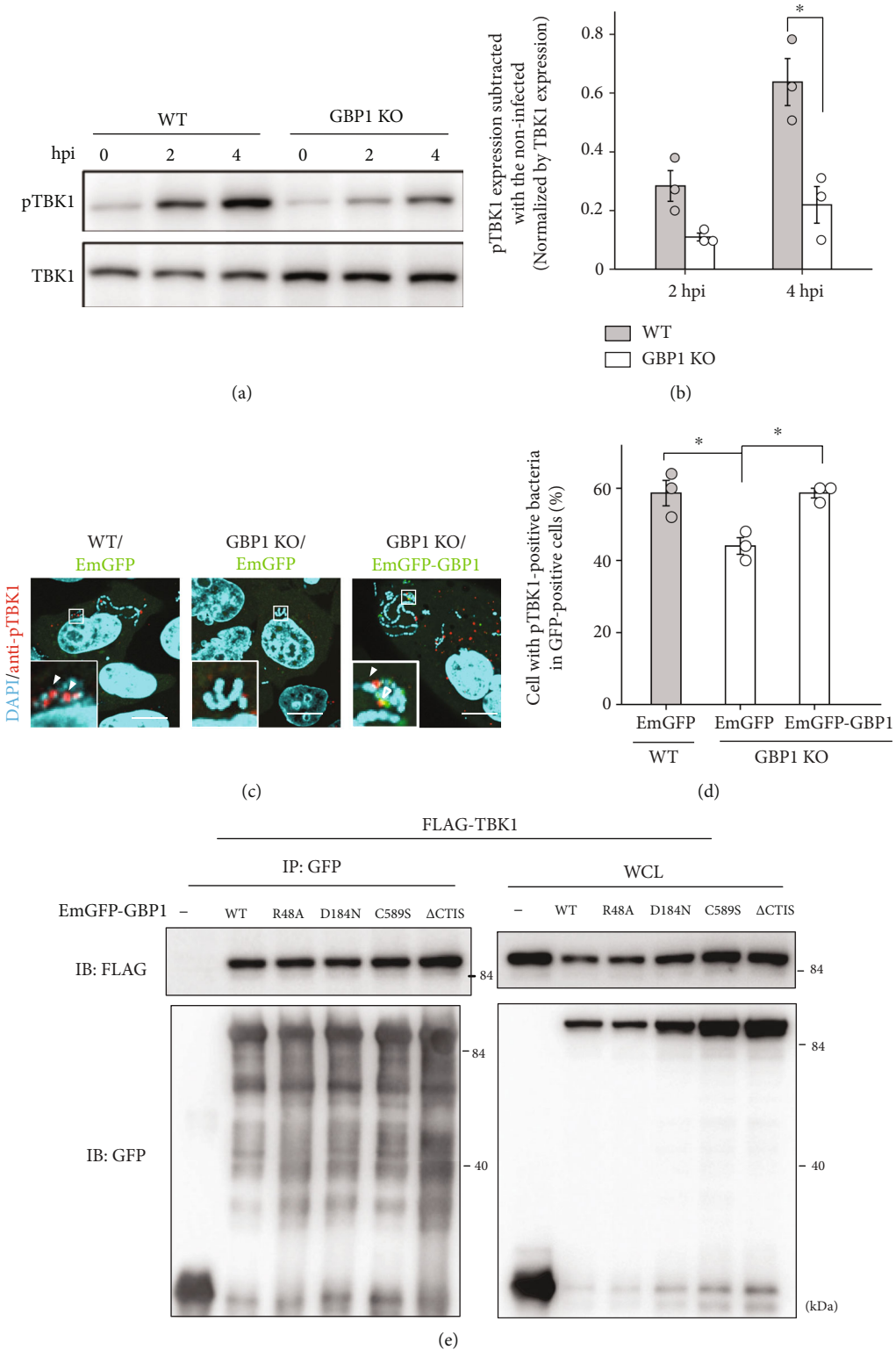

FIGURE 5: Continued.

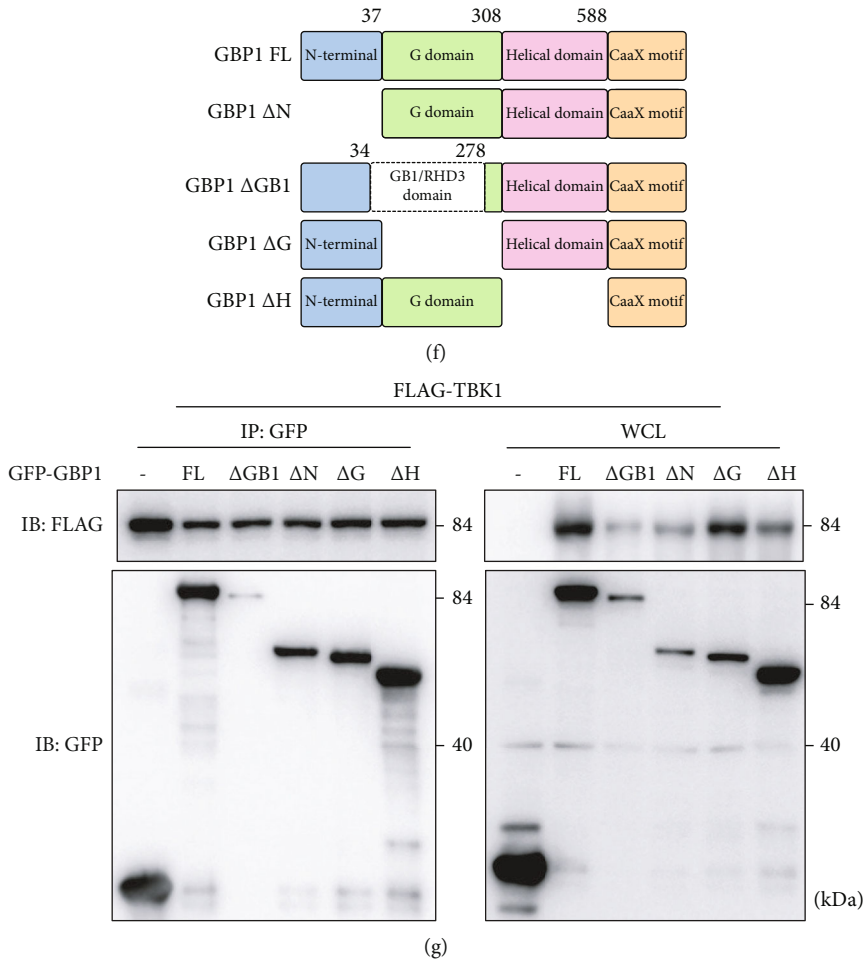

Figure 5: GBP1 interacts with TBK1 and regulates its phosphorylation. (a) Western blotting image of phosphorylated TBK1 (pTBK1) in HeLa WT and GBP1-KO cells during GAS infection. Cells were collected at the indicated time point. (b) Quantification of the pTBK1/TBK1 ratio in (a). Data are presented as the mean ± SD from three independent experiments. Asterisks indicate statistically significant differences ($^*p < 0.05$) as determined by two-tailed Student's *t*-test. (c) pTBK1 recruitment to GAS in HeLa WT and GBP1-KO cells. Cells were transfected with the indicated plasmids and then infected with GAS for 4 h. pTBK1 was colocalized with the bacteria (white outlined arrowhead) and GBP1 (white arrowhead). All images are representative of three independent experiments. Scale bar: 10 μm. (d) Percentage of cells containing pTBK1-positive GAS. Data are presented as the mean ± SD from three independent experiments (100 infected cells were examined in each experiment, counted manually using fluorescence microscopy). Asterisks indicate statistically significant differences ($^*p < 0.05$) as determined by two-tailed Student's *t*-test. (e) Immunoprecipitation of GFP-GBP1 intact or GBP1 mutants and FLAG-TBK1. Cells cotransfected with the indicated plasmids were subjected to immunoprecipitation using GFP-Trap. The immunoprecipitated proteins and total cell lysates were analyzed by immunoblotting with anti-GFP and anti-FLAG antibodies. (f) Schematic representation of intact GBP1 and mutants with deletion of different domains of GBP1. (g) Immunoprecipitation of GFP-GBP1 intact or mutants with deletion of GBP1 domains and FLAG-TBK1. Cells cotransfected with the indicated plasmids were subjected to immunoprecipitation using GFP-Trap. The immunoprecipitated proteins and total cell lysates were analyzed by immunoblotting with anti-GFP and anti-FLAG antibodies.

conclusion that GBP1 contributes to bacterial killing through xenophagy.

According to a previous report that described that GBP1 is essential for the recruitment of GBP2, GBP3, and GBP4 to *Shigella*, we examined the recruitment of GBP2 and GBP4 to GAS in GBP1-knockout cells. As shown in Supplementary Figure 1C, there was no difference between the WT and knockout cells. This suggests that the mechanism of recruitment of GBP2 and GBP4 differs between *Shigella* infection and GAS infection.

In *Chlamydia* infection, IFN-dependent suppression of bacterial infectivity requires both GBP1 and GBP2 [20]. To investigate the involvement of GBP2 in GAS growth suppression, we also established GBP2-knockout cells and infected the cells with bacteria. Unlike GBP1-knockout cells, GBP2-knockout cells showed no decrease in the rate of autophagosome formation (Supplementary Figure 1B). Taking this and the previous results together, it is suggested that GBP1 is a key regulator of GAS-induced autophagy in the human GBP family.

1.6. IFN Priming Does Not Affect Autophagosome Formation Response to GAS Infection. GBP1 is usually expressed at a low level in HeLa cells but is drastically upregulated by IFN-γ [36]. We hypothesized that GBP1 regulates autophagosome formation by its increased expression in response to GAS infection. However, the GBP1 expression level remained low, and its increase was not observed during GAS infection (data not shown). Moreover, IFN-γ-primed HeLa cells did not show any change in the rate of autophagosome formation (Supplementary Figure 5A), in contrast to the case upon *Chlamydia* infection [36]. These findings together demonstrate that the GBP1-mediated regulation of xenophagy is not dependent on the GBP1 expression level; specifically, GBP1 can exert its function even at a low expression level, without IFN-γ treatment.

1.7. GBP1 Regulates Autophagy Response to GAS Infection through p62 Recruitment. To analyze which step of the autophagy induction process involves GBP1, we observed the recruitment of autophagy-related molecules. Although the recruitment of ubiquitin and autophagy receptors such as NDP52, NBR1, and TAX1BP1 did not change, there was a clear reduction in p62 localization in GBP1-knockout cells at 2 h postinfection, an early stage of infection (Figures 4(a) and 4(b)). This reduction was recovered by intact GBP1 complementation (Figure 4(c)). GBP1 mutants with a deficiency in localization around GAS did not achieve the recovery of p62 recruitment, as for autophagosome formation (Figure 4(c)). This suggests that GBP1 contributes to autophagosome formation by recruiting p62 to the bacteria.

1.8. GBP1 Does Not Affect Lysophagy or Starvation-Induced Autophagy. Lysophagy, the autophagic degradation of lysosomes [37], and xenophagy, autophagy-mediated bacterial killing [38], share some molecular mechanisms. Because this study and a previous one [25] demonstrated that GBP1 is localized with galectin-3, a marker of membrane damage including ruptured lysosome [39] (Figure 2(f)), we considered the possibility that GBP1 also regulates lysophagy. One hour after LLOMe treatment, galectin-3 puncta were observed in HeLa WT cells (Figure 4(d)), which disappeared 10 h after the removal of LLOMe, suggesting lysophagic degradation. The same decrease was observed in GBP1-deleted cells. This suggests that GBP1 is not essential for lysophagy.

We also examined whether GBP1 is associated with nonselective autophagy because a previous report showed that p62-deleted cells accumulated LC3-positive puncta under starvation conditions, indicating the impairment of autophagic flux [40]. In wild-type HeLa cells stably expressing mCherry-LC3 [41], starvation-induced autophagy was seen in the form of LC3 puncta. The puncta were observed similarly even in GBP1-knockout cells (Figures 4(e) and 4(f)), suggesting that GBP1 is not required for starvation-induced autophagy. Taken together, our results indicate that GBP1 specifically regulates bacterial infection-induced autophagy, not starvation- and lysosomal damage-induced autophagy, through p62 recruitment.

1.9. GBP1 Promotes TBK1 Phosphorylation during GAS Infection. We next examined how GBP1 regulates p62 recruitment. TBK1 regulates the p62 localization response to cellular stresses such as mitochondrial damage and bacterial infection [42, 43], so we speculated that GBP1 is required for TBK1 function. TBK1 is activated by bacterial invasion and works as a kinase that phosphorylates serine 403 of p62 to promote interaction with molecules that have been ubiquitinated as a label, indicating that they are to be disassembled. To analyze TBK1 activation in GBP1 deletion mutant, we used immunoblotting to monitor the S172 phosphorylation of TBK1, which is critical for TBK1 activation [44]. Phosphorylated TBK1 (pTBK1) was shown to be upregulated under GAS infection in HeLa WT cells, although GBP1 deletion attenuated it (Figures 5(a) and 5(b)). This reduction was also seen in A549 cells (Supplementary Figures 4G and 4H). Moreover, we previously reported that pTBK1 recruitment around bacteria was increased by GAS-induced TBK1 phosphorylation [19]. GBP1 knockout significantly reduced pTBK1 localization around GAS, although this decline was recovered by the expression of GBP1 (Figures 5(c) and 5(d)). Furthermore, we found that GFP-GBP1 colocalized not only with bacteria (Figure 5(c), arrowhead) but also with pTBK1 around bacteria (Figure 5(c), open arrowhead). These results suggest that GBP1 regulates the TBK1 phosphorylation response to bacterial infection.

1.10. GBP1 Interacts with TBK1 Independently of Nucleotide Hydrolysis and Lipidation. Previous studies reported that the phosphorylation of TBK1 is mainly controlled by its localization, consequently triggering dimerization and trans-autophosphorylation upon stimulation [45]. Because the colocalization of pTBK1 and ectopically expressed GBP1 was observed, we speculated that GBP1 interacts with TBK1 and contributes to its phosphorylation. An immunoprecipitation assay revealed that EmGFP-GBP1 interacts with FLAG-TBK1 (Figures 5(e), 2 lanes on the left). This interaction was not interfered with GBP1 mutants unable to surround GAS (Figures 5(e), 4 lanes on the right). These results suggest that GBP1 regulates GAS-induced autophagy in two steps: interaction with TBK1 and localization to GAS, independently.

1.11. Mapping of the TBK1-Interacting Region of GBP1. Human GBP1 contains three main domains: an N-terminal domain (aa 1–37), a G-domain that is critical for nucleotide binding (aa 38–308), and a helical domain that is required for membrane binding and allosteric conformation (aa 309–588), along with one motif, the CAAX motif, which is prenylated and critical for membrane binding (Figure 5(f)). Additionally, one more region called the GB1/RHD3 domain is reported in the Protein Data Bank (PDB 1F5N), which is also important for guanine nucleotide binding and hydrolysis (aa 35–278, GB1) (Figure 5(f)). To determine the region responsible for TBK1-GBP1 interaction, we generated deletion mutants for each domain/motif. Immunoprecipitation assays revealed that this interaction was not affected for ΔG, ΔGB1, and ΔH (Figure 5(g)). Consistent

with these results, both G and helical domains showed somewhat faint but concrete interaction with TBK1 (Supplementary Figure 6A). These findings together demonstrate that a wide region of GBP1 is involved in the interaction with TBK1.

2. Discussion

In the present study, we demonstrate that several GBP family members colocalize with invading GAS, while GBP1 in particular is involved in autophagosome formation to engulf bacteria. Reports about GBPs' function against infection by Gram-negative bacteria have been published [10, 11, 46, 47]. However, few studies have investigated the dynamics of GBPs during infection with Gram-positive bacteria. A previous study reported that mouse GBP2 interacts with p62 and recruits ubiquitinated bacteria to autophagosomes during *Listeria* infection [5], but such function has not been reported for human GBPs, so their roles in human infection by Gram-positive bacteria remain incompletely understood. The present report, which focuses on the dynamics of human GBPs during GAS infection, contributes to our knowledge of the immune response to Gram-positive bacteria. Nevertheless, we examined GBP1 function only using cultured cells in this study. Further investigation using an animal model or human organoid resembling actual infectious conditions is still needed to clarify the function of GBP1 comprehensively.

We found that the localization of GBP1 around GAS is triggered by SLO, a pore-forming toxin secreted by bacteria, along with the recognition of membrane damage by galectin-3. As for the association of galectin-3 with the GBP family, a previous study demonstrated the interaction between mouse GBP2 and galectin-3 [25]. Meanwhile, another study reported that GBP1, GBP2, GBP3, and GBP4 localized with galectin-3-positive *Salmonella*, indicating that the rupture of bacterium-containing vacuoles is critical for GBP recruitment [47]. However, whether galectin-3 can regulate the localization of human GBPs remains to be elucidated. We demonstrated that the localization of human GBP1 is regulated by galectin-3 in a membrane damage-dependent manner, as shown in both GAS infection and LLOMe treatment. However, we have not yet clarified how galectin-3 recruits GBP1. In this paper, we demonstrated that GBP1 interacts with galectin-3, which is enhanced by GAS infection. Moreover, there is still a possibility that other galectins are involved in the regulation of GBP localization. Galectin-3, galectin-8, and galectin-9 have been reported to accumulate at damaged membranes associated with bacteria to overwhelm the infection [33, 48, 49]. We recently reported that galectin-1 and galectin-7 are also recruited to ruptured membranes around GAS and *Staphylococcus aureus* [50]. In this study, we demonstrated that GBP1 interacts with not only galectin-3 but also galectin-1, galectin-7, and galectin-8. It is worth examining whether GBP1 can integrate these galectins into bactericidal immune responses.

Our results showed that GBP1 was localized to GAS in a GTP hydrolysis-, GTP binding-, and prenylation-dependent manner. The mutants that did not localize to the bacteria could not complement p62 recruitment and autophagosome formation. These results suggest that the localization of GBP1 around the GAS is important for the recruitment of p62 and subsequent autophagosome formation. In addition, these results raise the possibility that GBP1 localization promotes the accumulation of phosphorylated TBK1 around the GAS, which regulates the localization of p62. Given the finding of a GBP1-TBK1 interaction in this study and the fact that this interaction is independent of GTP hydrolysis, GTP binding, and prenylation, there is a possibility that both the localization of GBP1 around GAS and GBP1-TBK1 interaction are required for GBP1-mediated autophagy. Since this study did not directly show the functional importance of the interaction between GBP1 and TBK1 for autophagosome formation, more detailed examination is needed in future work.

The localization of GBP1 around bacteria was critical for autophagosome formation, in contrast to the case for lysosome degradation (Figures 3(d) and 4(c)). This difference may be derived from the involvement of TBK1. In bacterial infection, autophagy receptors, including p62, are induced to undergo localization around the pathogen by TBK1. However, it has not been reported that TBK1 participates in p62 recruitment in lysosomal damage, which could explain why GBP1 deletion did not affect lysophagy [51, 52]. Moreover, the diversity of GBP1 function in selective autophagy suggests the variability of the autophagic pathway that remains to be elucidated. Additional studies to determine the roles of GBP family members in selective autophagy will be necessary to understand how they work downstream of membrane damage recognition.

GBP1 has a CAAX motif at its C-terminal, which is required for membrane binding, as is also the case for GBP2. However, despite the absence of CAAX motifs, GBP4 appears to localize at damaged membranes around GAS (Figure 1(a)). Studies have reported that GBP4 is recruited around *Shigella* and *Salmonella* in a manner dependent on GBP1, which binds to LPS [3, 10, 11, 46, 47]. Because GAS is a Gram-positive bacterium, GBP4 is thought to localize around GAS by a mechanism different from *Shigella* and *Salmonella*. One possible explanation for this is heterodimer formation. GBP4 can localize to vesicles in cells with the help of other GBPs with CAAX motifs [30]. In GAS infection, GBP4 may form a heterodimer with GBP1 or GBP2, GBP members with a CAAX motif, which then leads to the recruitment of GBP4 to the bacteria.

TBK1 works as a kinase activated by trans-autophosphorylation [45]. In selective autophagy, phosphorylated TBK1 facilitates the recruitment of receptor proteins to the object to be degraded [41, 42, 53], which consequently promotes engulfment by autophagosomes. In pathogenic infection, the causative agents of TBK1 phosphorylation were reported to be only bacterial remnants such as DNA, LPS, and their ligands in the host cells [18, 54, 55]. In this study, we demonstrate that GBP1, whose localization is regulated by recognizing membrane damage, interacts with TBK1 and enhances its phosphorylation. To the best of our knowledge, this is the first report suggesting the existence of a direct pathway from the identification of membrane damage to TBK1

phosphorylation. Intriguingly, we recently reported that TBK1 activation during GAS infection does require Ca^{2+}/TBC1D9 signaling, but not bacterial DNA sensing, which consequently recruits NDP52 through TBK1 phosphorylation [19]. Taking these findings together, it is suggested that host cells use different bacterial remnant-independent TBK1 activation pathways for each adaptor protein. Intriguingly, the Ca^{2+}/TBC1D9 axis affects not only NDP52 localization but also that of p62 [19]. Taking these findings together with our study, p62 recruitment to GAS may be regulated by several pathways, including the GBP1-TBK1 axis and the Ca^{2+}/TBC1D9 one. This may be why GBP1 knockout only partially affects p62 recruitment and subsequent autophagosome formation. In addition, neither GBP1 KO nor Ca^{2+}/TBC1D9 signaling depletion can completely inhibit adaptor protein recruitment, so the possibility of there being other pathways activating TBK1 remains.

In conclusion, we have demonstrated GBP1's involvement in xenophagy in a manner dependent on membrane damage recognition. We also showed that GBP1 regulates TBK1 phosphorylation and GBP1-TBK1 interaction. These findings provide new insights into patterns of immune response and may help elucidate therapeutic targets for infectious diseases.

3. Experimental Procedures

3.1. Cell Culture and Transfection. HeLa and A549 cells were purchased from American Type Culture Collection (ATCC). Cells were maintained in 5% CO_2 at 37°C in Dulbecco's modified Eagle's medium (Nacalai Tesque) supplemented with 10% fetal bovine serum (Gibco) and 50 μg/mL gentamicin (Nacalai Tesque). To induce starvation, cells were incubated in Dulbecco's modified Eagle's medium (Nacalai Tesque) without serum. Polyethylenimine (Polyscience) was used for transfection.

3.2. Group A Streptococcus. Group A *Streptococcus* strain JRS4 ($M6^+$ $F1^+$) was kindly provided by Dr. E. Hanski (Hebrew University, Israel). The bacteria were grown in Todd-Hewitt broth (BD Diagnostic Systems) supplemented with 0.2% yeast extract.

3.3. Reagents and Antibodies. The following antibodies were used: rat anti-human GBP1 (sc-53857; Santa Cruz Biotechnologies), mouse anti-galectin-3 (B2C10, 556904; BD Pharmingen), mouse anti-multi-ubiquitin (FK2, MFK-004; Nippon Bio-Test Laboratories), rabbit anti-TAX1BP1 (D1D5, 5105S; Cell Signaling Technology), rabbit anti-NBR1 (D2E6, 9891; Cell Signaling Technology), mouse anti-p62 (D-3, sc-28359; Santa Cruz), rabbit anti-Atg5 (D5F5U, 12994; Cell Signaling Technology), rabbit anti-TBK1 (EP611Y, ab40676; Abcam), rabbit anti-pTBK1/NAK (S172, D52C2; Cell Signaling Technology), mouse anti-GFP (GF200, 04363-24; Nacalai Tesque), and mouse anti-FLAG (M2, A2220; Sigma). The following reagents were used: $_L$-leucyl-$_L$-leucine methyl ester (LLOMe) (Cayman Chemical) and recombinant human IFN-γ (285-IF; RSD).

3.4. Plasmids. Human GBP1-7 was amplified by RT-PCR from HeLa total mRNA and cloned into pcDNA-6.2/N-EmGFP-DEST and pcDNA-6.2/N-3xFLAG-DEST using Gateway (Invitrogen) technology. The resulting constructs were N-terminally fused with corresponding tags. GBP1 was mutated by site-directed mutagenesis using the PrimeSTAR Mutagenesis Basal Kit (Takara).

3.5. Generation of Knockout Cell Lines Using the CRISPR/Cas9 Gene Editing System. ATG5-knockout and galectin-3-knockout HeLa cells had previously been established in our laboratory [41, 50]. GBP1-knockout A549 and ATG5-knockout HeLa and A549 cell lines were generated using the CRISPR/Cas9 gene editing system [56]. The designed gRNAs were cloned into the px459 vector (#62988; Addgene); the sequences were 5′-GCGGCAGCTACGGG GGATCC-3′ for ATG7, 5′-CATTACACAGCCTATG GTGG-3′ for HeLa GBP1-knockout cells, and 5′-TTTAGT GTGAGACTGCACCG-3′ for A549 GBP1-knockout cells. The vector was transfected into HeLa cells or A549 cells, and 48 h later, the cells were cultured in selection medium containing 2 μg/mL puromycin (Invivogen). Single colonies were picked up and cultured in 24-well plates; after expanding the cultures, deletion of the target gene was confirmed by immunoblotting and sequencing of the target loci.

3.6. Bacterial Infection. Cells were cultured in 24-well plates at a density of 4×10^4 cells/well for overexpression of the gene of interest or at 1×10^5 cells without gene manipulation. After replacing medium without antibiotics, cells were infected with GAS at a multiplicity of infection (MOI) of 100 for 1 h, washed with PBS, and cultured in medium containing 100 μg/mL gentamicin to kill the extracellular bacteria until the indicated time point of experimental use.

3.7. Fluorescence Microscopy. HeLa cells were plated on 0.1% gelatin-coated coverslips in 24-well plates. After GAS infection or the indicated treatment, cells were fixed with 4% paraformaldehyde for 15 min, washed with PBS, and permeabilized with 0.1% Triton X-100 in PBS for 10 min. After blocking with 2% BSA at room temperature for 1 h, cells were probed with a specific primary antibody diluted with blocking buffer at 4°C overnight, washed with PBS, and reacted with secondary antibody at room temperature for 2 h. Cellular and bacterial DNA was stained with 4′,6-diamidino-2-phenylindole (DAPI). Confocal micrographs were acquired using an FV1000 laser scanning microscope.

3.8. Bacterial Invasion and Viability Assays. A549 cells cultured at a density of 1×10^5 in 24-well plates were infected with GAS at an MOI of 10 for 1 h, as described in the previous section. Subsequently, cells were washed with PBS and cultured in medium containing 100 μg/mL gentamicin to kill extracellular bacteria before collecting the lysate. At 1, 2, and 6 h postinfection, cells were washed with PBS and lysed in sterile distilled water. Serial dilutions of the lysates were plated on tryptic soy broth agar plates. The bacterial invasion rate was calculated as the ratio of intracellular bacteria at 2 h postinfection to cell-attached bacteria at 1 h

postinfection. The GAS growth ratio was determined as the ratio of intracellular bacteria at 6 h postinfection to that at 2 h postinfection.

3.9. Immunoprecipitation. For immunoprecipitation assays, cells were transfected with the indicated plasmids using a polyethylenimine reagent and harvested 2 days later. After washing with PBS, cells were collected and lysed with buffer containing 10 mM Tris-HCl (pH 7.4), 1% NP-40, 150 mM NaCl, 1 mM ethylenediaminetetraacetic acid (EDTA), 5% glycerol, and proteinase-inhibitor cocktail (Nacalai Tesque). Lysates were centrifuged at 15,000 rpm for 20 min, and the supernatant was incubated with GFP-trap Agarose (Chromotek) for 1 h at 4°C. Subsequently, the beads were washed five times with lysis buffer and the immunoprecipitants were eluted with 2× Laemmli sample buffer. For immunoblotting, proteins were separated using SDS-PAGE, transferred to PVDF membranes, and detected using specific primary antibodies with overnight incubation at 4°C, followed by labeling with an appropriate secondary antibody.

Data Availability

The data used to support the findings of this study are available from the corresponding author upon request.

Conflicts of Interest

The authors declare that they have no conflicts of interest.

Authors' Contributions

M.H., T.N., and I.N. designed the study. M.H., H.T., A.M.N., and T.N. performed the experiments. M.H. analyzed the data. M.H. wrote the manuscript after fruitful discussions with and under the supervision of T.N. and I.N.

Acknowledgments

We thank Edanz (https://jp.edanz.com/ac) for editing the English text of a draft of this manuscript. This work was supported in part by a Grant-in-Aid for JSPS Fellows (21J15169), by Grants-in-Aid for Scientific Research (18K07109, 21K07023, 21K19376, 19H03471, 22H02868, 22H, and 22H04809), by the Takeda Science Foundation (to T.N.), by the Chemo-Sero-Therapeutic Research Institute (to T.N.), by AMED (Grant Number JP22fk0108130h0403, to I.N.), by the Grants-in-Aid for Research from the Japan Racing and Livestock Promotion Foundation (to I.N.), by the Joint Research Project of the Institute of Medical Science, the University of Tokyo (to I.N.), by the Yakult Foundation (to I.N.), by the Research Center for GLOBAL and LOCAL Infectious Diseases, Oita University (2021B15) (to I.N.), by the Grants-in-Aid for Research from the National Center for Global Health and Medicine (22A1016), and by the Grants-in-Aid for Research from Chemo-Sero-Therapeutic Research Institute (to I.N.).

Supplementary Materials

Supplementary 1. Supplementary Figure 1: dynamics of GBP2 and GBP4 on autophagosome formation. (A) Quantification of GBP2 and GBP4 recruitment in HeLa WT and galectin-3-KO cells. (B) Autophagosome formation rate in HeLa WT and GBP2-KO cells. (C) GBP2 and GBP4 recruitment ratio in HeLa WT and GBP1-KO cells. Data are presented as the mean ± SD from three or four independent experiments (>50 infected cells were manually counted in each experiment).

Supplementary 2. Supplementary Figure 2: GBP1 interacts with galectins. (A) Immunoprecipitation of FLAG-GBP1 and GFP-galectins. Cells cotransfected with the indicated plasmids were subjected to immunoprecipitation using GFP-Trap. The immunoprecipitated proteins and total cell lysates were analyzed by immunoblotting with anti-GFP and anti-FLAG antibodies.

Supplementary 3. Supplementary Figure 3: GBP1 deletion affects autophagosome maturation, following autophagosome formation. (A) Recruitment of LAMP1 around GAS in HeLa WT and GBP1-KO cells. Cells were transfected with EmGFP or EmGFP-GBP1 and infected with GAS for 4 h. After fixation, cells were stained with a LAMP1 antibody. An overview of the merging of all channels and a magnified view of it are shown. All images are representative of three independent experiments. Scale bar: 10 μm. (B) LAMP1-positive rate in GAS-infected cells. Data are presented as the mean ± SD from three independent experiments (50 infected cells were manually counted in each experiment). Asterisks indicate statistically significant differences ($^{*}p < 0.05$, $^{**}p < 0.01$) as determined by two-tailed Student's t-test.

Supplementary 4. Supplementary Figure 4: A549 GBP1-KO cells show a phenotype similar to that of HeLa GBP1-KO cells. (A) Confocal micrographs of the GBP family around an autophagosome in GAS-infected cells. A549 cells expressing the indicated EmGFP-GBPs (green) and mCherry-LC3 (red) were infected with GAS for 4 h. Cellular and bacterial DNA was stained with DAPI (cyan). Insets: enlargements of the indicated areas. Scale bar: 5 μm. (B) Western blotting images of A549 WT and GBP1-KO cells. Cells were incubated in 10 ng/mL IFN-γ-containing medium for 24 h. (C) Sequence alignment of A549 WT and GBP1-KO cell lines. The query is human GBP1 CDS (NCBI accession number: *Homo sapiens* guanylate binding protein 1, mRNA, NM_002053.3). (D) Western blotting images of A549 WT and ATG5-KO cells. (E) Viability of GAS in A549 WT, GBP1-KO #2, and ATG5-KO cells. Triplicate samples were used in each experiment, and colonies were counted manually. Data are presented as the mean ± SD from four independent experiments. Asterisks indicate statistically significant differences ($^{*}p < 0.05$) as determined by two-tailed Student's t-test. The same data of GBP1 KO #1 are shown in Supplementary Figure 2D. (F) Autophagosome formation rate of GBP1-KO A549 cells. Cells were transfected with

mCherry-LC3, as an autophagosome marker, and EmGFP or EmGFP-GBP1. Data are presented as the mean ± SD from three independent experiments (100 infected cells were manually counted in each experiment). Asterisks indicate statistically significant differences ($^*p < 0.05$) as determined by two-tailed Student's t-test. (G) Western blotting image of pTBK1 in A549 WT and GBP1-KO cell lines during GAS infection. Cells were collected at the indicated time point. (H) Quantification of the pTBK1/TBK1 ratio in (F). Data are presented as the mean ± SD from three independent experiments. Asterisks indicate statistically significant differences ($^*p < 0.05$) as determined by two-tailed Student's t-test.

Supplementary 5. Supplementary Figure 5: IFN priming does not affect autophagosome formation during GAS infection. (A) Rate of autophagosome formation in naïve and IFN-γ-primed HeLa cells. Cells were transfected with mCherry-LC3 as an autophagosome marker and then infected with GAS for 4 h. Under primed conditions, cells were incubated in 1 ng/mL IFN-γ-containing medium for at least 16 h before GAS infection. Data are presented as the mean ± SD from three independent experiments (100 infected cells were manually counted in each experiment).

Supplementary 6. Supplementary Figure 6: single domain of GBP1 interacts with TBK1. (A) Immunoprecipitation of EmGFP-GBP1 intact or GBP1 deletion mutants and FLAG-TBK1. Cells cotransfected with the indicated plasmids were subjected to immunoprecipitation using GFP-Trap. The immunoprecipitated proteins and total cell lysates were analyzed by immunoblotting with anti-GFP and anti-FLAG antibodies.

References

[1] G. Kak, M. Raza, and B. K. Tiwari, "Interferon-gamma (IFN-γ): exploring its implications in infectious diseases," *Biomolecular Concepts*, vol. 9, no. 1, pp. 64–79, 2018.

[2] F. Mcnab, K. Mayer-barber, A. Sher, A. Wack, and A. O. Garra, "Type I interferons in infectious disease," *Nature Reviews. Immunology*, vol. 15, no. 2, pp. 87–103, 2015.

[3] M. Kutsch, L. Sistemich, C. F. Lesser, M. B. Goldberg, C. Herrmann, and J. Coers, "Direct binding of polymeric GBP1 to LPS disrupts bacterial cell envelope functions," *The EMBO Journal*, vol. 39, no. 13, pp. 1–22, 2020.

[4] K. Tretina, E. S. Park, A. Maminska, and J. D. MacMicking, "Interferon-induced guanylate-binding proteins: guardians of host defense in health and disease," *The Journal of Experimental Medicine*, vol. 216, no. 3, pp. 482–500, 2019.

[5] B.-H. Kim, A. R. Shenoy, P. Kumar, R. Das, S. Tiwari, and J. D. MacMicking, "A family of IFN-γ–inducible 65-kD GTPases Protects against bacterial infection," *Science*, vol. 332, no. 6030, pp. 717–721, 2011.

[6] D. Fisch, B. Clough, M. C. Domart et al., "Human GBP1 differentially targets Salmonella and Toxoplasma to license recognition of microbial ligands and caspase-mediated death," *Cell Reports*, vol. 32, no. 6, article 108008, 2020.

[7] A. M. P. dos Santos, R. G. Ferrari, and C. A. Conte-Junior, "Type three secretion system in Salmonella typhimurium: the key to infection," *Genes and Genomics*, vol. 42, no. 5, pp. 495–506, 2020.

[8] M. P. Wandel, B. H. Kim, E. S. Park et al., "Guanylate-binding proteins convert cytosolic bacteria into caspase-4 signaling platforms," *Nature Immunology*, vol. 21, no. 8, pp. 880–891, 2020.

[9] P. Li, W. Jiang, Q. Yu et al., "Ubiquitination and degradation of GBPs by a Shigella effector to suppress host defence," *Nature*, vol. 551, no. 7680, pp. 378–383, 2017.

[10] A. S. Piro, D. Hernandez, S. Luoma et al., "Detection of cytosolic Shigella flexneri via a C-terminal triple-arginine motif of GBP1 inhibits actin-based motility," *MBio*, vol. 8, no. 6, pp. 1–16, 2017.

[11] M. P. Wandel, C. Pathe, E. I. Werner et al., "GBPs inhibit motility of Shigella flexneri but are targeted for degradation by the bacterial ubiquitin ligase IpaH9.8," *Cell Host & Microbe*, vol. 22, no. 4, pp. 507–518.e5, 2017.

[12] N. Mizushima and M. Komatsu, "Autophagy: renovation of cells and tissues," *Cell*, vol. 147, no. 4, pp. 728–741, 2011.

[13] H. Morishita and N. Mizushima, "Diverse cellular roles of autophagy," *Annual Review of Cell and Developmental Biology*, vol. 35, no. 1, pp. 453–475, 2019.

[14] A. J. Perrin, X. Jiang, C. L. Birmingham, N. S. Y. So, and J. H. Brumell, "Recognition of bacteria in the cytosol of mammalian cells by the ubiquitin system," *Current Biology*, vol. 14, no. 9, pp. 806–811, 2004.

[15] A. Huett, R. J. Heath, J. Begun et al., "The LRR and RING domain protein LRSAM1 is an E3 ligase crucial for ubiquitin-dependent autophagy of intracellular Salmonella typhimurium," *Cell Host & Microbe*, vol. 12, no. 6, pp. 778–790, 2012.

[16] E. G. Otten, E. Werner, A. Crespillo-Casado et al., "Ubiquitylation of lipopolysaccharide by RNF213 during bacterial infection," *Nature*, vol. 594, no. 7861, pp. 111–116, 2021.

[17] Z. Wang and C. Li, "Xenophagy in innate immunity: a battle between host and pathogen," *Developmental and Comparative Immunology*, vol. 109, article 103693, 2020.

[18] R. O. Watson, S. L. Bell, D. A. MacDuff et al., "The cytosolic sensor cGAS detects Mycobacterium tuberculosis DNA to induce type I interferons and activate autophagy," *Cell Host & Microbe*, vol. 17, no. 6, pp. 811–819, 2015.

[19] T. Nozawa, S. Sano, A. Minowa-Nozawa et al., "TBC1D9 regulates TBK1 activation through Ca2+ signaling in selective autophagy," *Nature Communications*, vol. 11, no. 1, pp. 1–16, 2020.

[20] M. A. Al-Zeer, H. M. Al-Younes, D. Lauster, M. A. Lubad, and T. F. Meyer, "Autophagy restricts Chlamydia trachomatis growth in human macrophages via IFNG-inducible guanylate binding proteins," *Autophagy*, vol. 9, no. 1, pp. 50–62, 2013.

[21] A. C. Johnston, A. Piro, B. Clough et al., "Human GBP1 does not localize to pathogen vacuoles but restricts Toxoplasma gondii," *Cellular Microbiology*, vol. 18, no. 8, pp. 1056–1064, 2016.

[22] J. N. Cole, T. C. Barnett, V. Nizet, and M. J. Walker, "Molecular insight into invasive group A streptococcal disease," *Nature Reviews. Microbiology*, vol. 9, no. 10, pp. 724–736, 2011.

[23] I. Nakagawa, A. Amano, N. Mizushima et al., "Autophagy defends cells against invading group AStreptococcus," *Science*, vol. 306, no. 5698, pp. 1037–1040, 2004.

[24] C. C. Ngo and S. M. Man, "Mechanisms and functions of guanylate-binding proteins and related interferon-inducible GTPases: roles in intracellular lysis of pathogens," *Cellular Microbiology*, vol. 19, no. 12, pp. 1–9, 2017.

[25] E. M. Feeley, D. M. Pilla-Moffett, E. E. Zwack et al., "Galectin-3 directs antimicrobial guanylate binding proteins to vacuoles furnished with bacterial secretion systems," *Proceedings of the National Academy of Sciences of the United States of America*, vol. 114, no. 9, pp. E1698–E1706, 2017.

[26] G. J. K. Praefcke, M. Geyer, M. Schwemmle, H. Robert Kalbitzer, and C. Herrmann, "Nucleotide-binding characteristics of human guanylate-binding protein 1 (hGBP1) and identification of the third GTP-binding motif," *Journal of Molecular Biology*, vol. 292, no. 2, pp. 321–332, 1999.

[27] G. J. K. Praefcke, S. Kloep, U. Benscheid, H. Lilie, B. Prakash, and C. Herrmann, "Identification of residues in the human guanylate-binding protein 1 critical for nucleotide binding and cooperative GTP hydrolysis," *Journal of Molecular Biology*, vol. 344, no. 1, pp. 257–269, 2004.

[28] A. Xavier, M. A. Al-Zeer, T. F. Meyer, and O. Daumke, "hGBP1 coordinates chlamydia restriction and inflammasome activation through sequential GTP hydrolysis," *Cell Reports*, vol. 31, no. 7, article 107667, 2020.

[29] N. Modiano, Y. E. Lu, and P. Cresswell, "Golgi targeting of human guanylate-binding protein-1 requires nucleotide binding, isoprenylation, and an IFN-γ-inducible cofactor," *Proceedings of the National Academy of Sciences*, vol. 102, no. 24, pp. 8680–8685, 2005.

[30] N. Britzen-Laurent, M. Bauer, V. Berton et al., "Intracellular trafficking of guanylate-binding proteins is regulated by heterodimerization in a hierarchical manner," *PLoS One*, vol. 5, no. 12, p. e14246, 2010.

[31] D. Fisch, H. Bando, B. Clough et al., "Human GBP1 is a microbe-specific gatekeeper of macrophage apoptosis and pyroptosis," *The EMBO Journal*, vol. 38, no. 13, pp. 1–19, 2019.

[32] A. K. Haldar, A. S. Piro, D. M. Pilla, M. Yamamoto, and J. Coers, "The E2-like conjugation enzyme Atg3 promotes binding of IRG and Gbp proteins to Chlamydia- and Toxoplasma-containing vacuoles and host resistance," *PLoS One*, vol. 9, no. 1, 2014.

[33] S. Chauhan, S. Kumar, A. Jain et al., "TRIMs and galectins globally cooperate and TRIM16 and galectin-3 co-direct autophagy in endomembrane damage homeostasis," *Developmental Cell*, vol. 39, no. 1, pp. 13–27, 2016.

[34] J. Hasegawa, I. Maejima, R. Iwamoto, and T. Yoshimori, "Selective autophagy: lysophagy," *Methods*, vol. 75, pp. 128–132, 2015.

[35] N. Mizushima, A. Yamamoto, M. Hatano et al., "Dissection of autophagosome formation using Apg5-deficient mouse embryonic stem cells," *The Journal of Cell Biology*, vol. 152, no. 4, pp. 657–668, 2001.

[36] I. Tietzel, C. El-Haibi, and R. A. Carabeo, "Human guanylate binding proteins potentiate the anti-chlamydia effects of interferon-γ," *PLoS One*, vol. 4, no. 8, p. e6499, 2009.

[37] C. Papadopoulos, B. Kravic, and H. Meyer, "Repair or lysophagy: dealing with damaged lysosomes," *Journal of Molecular Biology*, vol. 432, no. 1, pp. 231–239, 2020.

[38] W. Hu, H. Chan, L. Lu et al., "Autophagy in intracellular bacterial infection," *Seminars in Cell & Developmental Biology*, vol. 101, pp. 41–50, 2020.

[39] I. Maejima, A. Takahashi, H. Omori et al., "Autophagy sequesters damaged lysosomes to control lysosomal biogenesis and kidney injury," *The EMBO Journal*, vol. 32, no. 17, pp. 2336–2347, 2013.

[40] G. Bjørkøy, T. Lamark, A. Brech et al., "p62/SQSTM1 forms protein aggregates degraded by autophagy and has a protective effect on huntingtin-induced cell death," *The Journal of Cell Biology*, vol. 171, no. 4, pp. 603–614, 2005.

[41] A. Minowa-Nozawa, T. Nozawa, K. Okamoto-Furuta, H. Kohda, and I. Nakagawa, "Rab35 GTPase recruits NDP52 to autophagy targets," *The EMBO Journal*, vol. 36, no. 18, article e201796463, pp. 2790–2807, 2017.

[42] G. Matsumoto, T. Shimogori, N. Hattori, and N. Nukina, "TBK1 controls autophagosomal engulfment of polyubiquitinated mitochondria through p62/SQSTM1 phosphorylation," *Human Molecular Genetics*, vol. 24, no. 15, pp. 4429–4442, 2015.

[43] M. Pilli, J. Arko-Mensah, M. Ponpuak et al., "TBK-1 promotes autophagy-mediated antimicrobial defense by controlling autophagosome maturation," *Immunity*, vol. 37, no. 2, pp. 223–234, 2012.

[44] N. Kishore, Q. K. Huynh, S. Mathialagan et al., "IKK-i and TBK-1 are enzymatically distinct from the homologous enzyme IKK-2. Comparative analysis of recombinant human IKK-i, TBK-1, and IKK-2," *The Journal of Biological Chemistry*, vol. 277, no. 16, pp. 13840–13847, 2002.

[45] E. Helgason, Q. T. Phung, and E. C. Dueber, "Recent insights into the complexity of Tank-binding kinase 1 signaling networks: the emerging role of cellular localization in the activation and substrate specificity of TBK1," *FEBS Letters*, vol. 587, no. 8, pp. 1230–1237, 2013.

[46] D. Fisch, H. Bando, B. Clough et al., "Human GBP 1 is a microbe-specific gatekeeper of macrophage apoptosis and pyroptosis," *The EMBO Journal*, vol. 38, no. 13, p. e100926, 2019.

[47] J. C. Santos, D. Boucher, L. K. Schneider et al., "Human GBP1 binds LPS to initiate assembly of a caspase-4 activating platform on cytosolic bacteria," *Nature Communications*, vol. 11, no. 1, p. 3276, 2020.

[48] I. Paz, M. Sachse, N. Dupont et al., "Galectin-3, a marker for vacuole lysis by invasive pathogens," *Cellular Microbiology*, vol. 12, no. 4, pp. 530–544, 2010.

[49] T. L. M. Thurston, M. P. Wandel, N. Von Muhlinen, Á. Foeglein, and F. Randow, "Galectin 8 targets damaged vesicles for autophagy to defend cells against bacterial invasion," *Nature*, vol. 482, no. 7385, pp. 414–418, 2012.

[50] C. Y. Lin, T. Nozawa, A. Minowa-Nozawa, H. Toh, C. Aikawa, and I. Nakagawa, "LAMTOR2/LAMTOR1 complex is required for TAX1BP1-mediated xenophagy," *Cellular Microbiology*, vol. 21, no. 4, pp. 1–15, 2019.

[51] C. Bussi, J. M. Peralta Ramos, D. S. Arroyo et al., "Alpha-synuclein fibrils recruit TBK1 and OPTN to lysosomal damage sites and induce autophagy in microglial cells," *Journal of Cell Science*, vol. 131, pp. 1–19, 2018.

[52] C. Papadopoulos and H. Meyer, "Detection and clearance of damaged lysosomes by the endo-lysosomal damage response and lysophagy," *Current Biology*, vol. 27, no. 24, pp. R1330–R1341, 2017.

[53] B. Richter, D. A. Sliter, L. Herhaus et al., "Phosphorylation of OPTN by TBK1 enhances its binding to Ub chains and promotes selective autophagy of damaged mitochondria," *Proceedings of the National Academy of Sciences*, vol. 113, no. 15, pp. 4039–4044, 2016.

[54] C. Zhao and W. Zhao, "TANK-binding kinase 1 as a novel therapeutic target for viral diseases," *Expert Opinion on Therapeutic Targets*, vol. 23, no. 5, pp. 437–446, 2019.

[55] H. Häcker and M. Karin, "Regulation and function of IKK and IKK-related kinases," *Science's STKE*, vol. 2006, no. 357, 2006.

[56] P. Mali, L. Yang, K. M. Esvelt et al., "RNA-guided human genome engineering via Cas9," *Science*, vol. 339, no. 6121, pp. 823–826, 2013.

[57] A. Minowa-Nozawa, T. Nozawa, K. O. Furuta, H. Kohda, and I. Nakagawa, "The Rab35 GTPase marks targets of the autophagosome by recruiting NDP52 Appendix Figures S1-S6," *The EMBO Journal*, 2018.